Q. J. R. Meteorol. Soc. (2005), **131**, pp. 1539–1565 doi: 10.1256/qj.04.94

Review of the vapour pressures of ice and supercooled water for atmospheric applications

By D. M. MURPHY*[1] and T. KOOP[2]

[1]*Aeronomy Laboratory, National Oceanic and Atmospheric Administration, Boulder, USA*
[2]*University of Bielefeld, Faculty of Chemistry, Germany*

(Received 16 June 2004 Revised 30 December 2004)

SUMMARY

The vapour pressures of ice and supercooled water are reviewed with an emphasis on atmospheric applications. Parametrizations are given for the vapour pressure, molar heat capacity, and latent heat of vaporization of both ice and liquid water. For ice, the experimental vapour pressure data are in agreement with a derivation from the Clapeyron equation. Below 200 K cubic ice may affect the vapour pressure of ice both in the atmosphere and in the laboratory. All of the commonly used parametrizations for the vapour pressure of supercooled water are extrapolations that were not originally intended for use below the freezing point. In addition, the World Meteorological Organization definition of the vapour pressure of supercooled water contains an easily overlooked typographical error. Recent data on the molar heat capacity of supercooled water are used to derive its vapour pressure. Nevertheless, the uncertainty is such that measurements of the deliquescence and freezing behaviour of aerosol particles are beginning to be limited by uncertainties in the thermodynamics of supercooled water.

KEYWORDS: Clapeyron equation Cubic ice Hexagonal ice Parametrizations Thermodynamics

1. INTRODUCTION

The vapour pressure of water over ice and supercooled water is important for cirrus clouds, polar stratospheric clouds, and for the great volume of the atmosphere that is colder than 273 K. The difference in vapour pressure over ice and over supercooled water is important for the growth of ice crystals in mixed-phase clouds. The composition and water uptake of deliquesced aerosol particles depend on the aqueous solution water activity, which is closely related to the vapour pressure of supercooled water.

How well do the vapour pressures of water and ice need to be specified for atmospheric applications? It is doubtful if any measurements of relative humidity in the atmosphere are sufficiently accurate in both water vapour and temperature to achieve 0.1% absolute accuracy. Water vapour measurements in the stratosphere have uncertainties of about 10%, with frost-point measurements consistently yielding results somewhat lower than other techniques (Kley *et al.* 2000). The uncertainties in the vapour pressure of ice and supercooled water are both greater than 0.1% except very close to the triple point. Physical processes (discussed below) in addition to the vapour pressure of bulk samples of pure water also come into play at about the 0.1% level.

There are several reasons for a new review of the vapour pressure of ice for atmospheric applications. First, none of the major expressions has been compared to measurements by Marti and Mauersberger (1993), which are probably the best experimental data below 205 K. Second, some of the parametrizations do not extend down to temperatures important in the stratosphere and mesosphere; for example, minimum temperatures in the Antarctic winter stratosphere can be below 175 K. Finally, metastable forms of ice such as cubic ice that may be important at temperatures below 200 K (Murphy 2003) have not been included in previous expressions.

The first modern derivation of the vapour pressure of ice was by Goff and Gratch (1946). It was later updated to revised temperature scales (Goff 1957, 1965). Hyland and

* Corresponding author: Aeronomy Laboratory, National Oceanic and Atmospheric Administration, Boulder, CO, USA. e-mail: daniel.m.murphy@noaa.gov

Wexler (1983) is another widely used derivation from much of the same thermodynamic data. The parametrization of Wagner *et al.* (1994) is approved by the International Association for the Properties of Water and Steam. The functional form was chosen to satisfy experimental constraints at the triple point as well as to have well-behaved derivatives. A broader approach is to fit master thermodynamic functions for ice and vapour that simultaneously satisfy experimental data not only for vapour pressure and latent heat but also for other properties such as the speed of sound (Wagner and Pruss 2002; Feistel and Wagner 2005). The vapour pressure derived from the master functions will automatically be self-consistent with other properties. Many other formulae for the vapour pressure of ice have been published: Washburn (1924) is historically important; Jancso *et al.* (1970) combines experimental and thermodynamic data; Buck (1981) is primarily an attempt to find more convenient mathematical forms rather than an independent derivation. See appendix A for a compilation of many of these expressions.

Surprisingly, none of the expressions commonly used for the vapour pressure of supercooled water were intended for that purpose in the original papers. According to Goff (1957), the International Meteorological Organization decided in 1947 to extrapolate the 1946 Goff–Gratch formula 'for undercooled liquid down to −50 °C pending further research'. Other derivations of the vapour pressure of water (Wexler 1977; Hyland and Wexler 1983; Wagner and Pruss 1993, 2002) are also stated by their authors as valid only above either the freezing or triple point; Sonntag (1990) is an update of Hyland and Wexler; McDonald (1965) is a restatement of Goff (1957; see appendix B).

2. Thermodynamic basis of the vapour pressure of ice

(*a*) *Clapeyron equation*

The vapour pressure of both ice and liquid water at the triple point is $p_t = 611.657 \pm 0.01$ Pa at temperature $T_t = 273.16$ K (Guildner *et al.* 1976). The high accuracy of this measured value will be used as a boundary condition. The vapour pressure may be extended down in temperature from the triple point using the Clapeyron equation:

$$\frac{\mathrm{d}p}{\mathrm{d}T} = \frac{\Delta s}{\Delta v}, \tag{1a}$$

where Δs and Δv are the molar entropy and volume changes upon sublimation, respectively.

To a very good approximation (discussed later), one may assume that the molar volume of ice is much less than that of water vapour, and that water vapour is an ideal gas. This is the Clausius–Clapeyron equation:

$$\frac{\mathrm{d}\ln p}{\mathrm{d}T} = \frac{L_{\mathrm{ice}}(T)}{RT^2}, \tag{1b}$$

where $L_{\mathrm{ice}}(T)$ is the latent heat of sublimation of ice as a function of temperature and R is the molar gas constant (8.31447 J mol^{-1}K^{-1}).

A useful starting point is to solve Eq. (1b) with L_{ice} approximated as constant. Then it can be easily evaluated to obtain a straight line for $\ln(p)$ versus $1/T$. Inserting numerical values for the vapour pressure and latent heat at the triple point (see below) along with a small adjustment for non-ideal behaviour gives:

$$p_{\mathrm{ice}} \approx \exp(28.9074 - 6143.7/T), \tag{2}$$

with temperature in K and pressure in Pa.

This functional form was used by Jancso *et al.* (1970), Marti and Mauersberger (1993), and Mauersberger and Krankowsky (2003) to fit experimental vapour pressure data (see appendix A).

The next level of detail beyond Eq. (2) is to include the temperature dependence of L_{ice}. This may be done by writing it as a function of $\Delta c_p(T)$, the difference in molar heat capacities of water vapour and ice (Pruppacher and Klett 1997):

$$L_{\text{ice}}(T) = L_{\text{ice,t}} + \int_{T_t}^{T} \Delta c_p(T')\,\mathrm{d}T' + \int_{T_t}^{T} \frac{\mathrm{d}p}{\mathrm{d}T'} \left\{ (v_v - v_i) - T' \left(\frac{\partial (v_v - v_i)}{\partial T'} \right)_p \right\} \mathrm{d}T', \tag{3}$$

where $L_{\text{ice,t}}$ is the latent heat of vaporization at the triple point T_t, Δc_p is the difference in molar heat capacities, and v_v and v_i are the molar volumes of vapour and ice. The second integral is very small compared to the first (it is zero for an ideal gas with $v_v \gg v_i$). However, it was included in the numerical integrations that form the basis for Eq. (7).

The value used here for $L_{\text{ice,t}}$ is 51059 J mol^{-1}. This is obtained by interpolating between measured values at 0 and 1 °C (Osborne *et al.* 1939; Osborne 1939). The smooth fit proposed by Osborne *et al.* and a value obtained from the difference of master thermodynamic functions for water vapour and ice (Wagner and Pruss 2002; Feistel and Wagner 2005) differ by up to 10 J mol^{-1}, but the true uncertainty may be larger because the values are not independent of each other. A molar mass of 18.015 g mol^{-1} for water was used when required to convert heat-capacity units.

(*b*) *Molar heat capacity*

Figure 1 shows the isobaric molar heat capacity, c_p, of ice and water vapour. Both sets of ice data are measurements. The Giauque and Stout (1936) data have been corrected for a change in definition of the calorie from 4.1832 to 4.184 J. Molar heat capacities of water vapour from Friedman and Haar (1954) are ideal-gas calculations from vibrational spectroscopy, and those from Wagner and Pruss (2002) are calculations from their thermodynamic function for water. Note that the molar heat capacities of ice and water vapour are of similar magnitude between 210 and 270 K. This is what makes the simple solution (Eq. (2)) work fairly well: the integral of Δc_p over 210–273 K is close to zero.

In units of J mol^{-1}K^{-1}, the molar heat capacity of ice can be fitted to within the scatter of the Giauque and Stout (1936) data by

$$c_{p,\text{ice}} = -2.0572 + 0.14644T + 0.06163T \exp\{-(T/125.1)^2\}, \quad T > 20\ \text{K}. \tag{4}$$

The last term is good for fitting the nonlinear portion because it goes to zero at both low and high temperatures, and can be integrated analytically. The same form can be used for the difference in heat capacity between vapour and ice. Using Wagner and Pruss (2002) for vapour, the coefficients are −35.319, 0.14457, 0.06155, 129.85. Because temperatures above 160 K are most important for the atmosphere, points below 160 K in this fit were weighted by 50% as much as points above 160 K, and points below 40 K 30% as much as points above 160 K.

Ignoring the second integral in Eq. (3), this expression for the difference in molar heat capacity integrates analytically to give the latent heat of sublimation of ice.

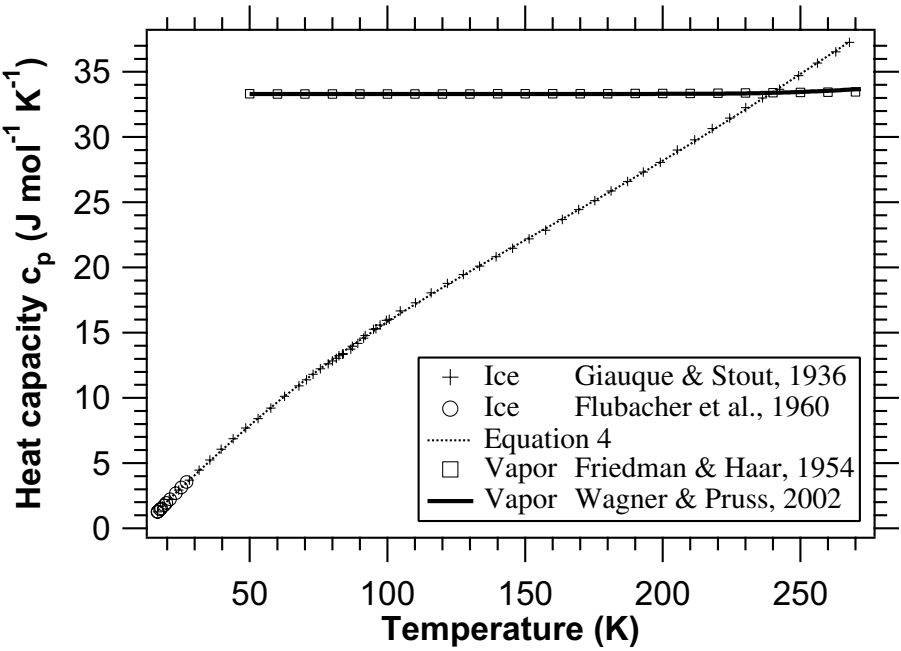

Figure 1. The molar heat capacities of ice and water vapour. The vapour-phase heat capacities from Wagner and Pruss (2002) include non-ideal-gas effects but those from Friedman and Haar (1954) do not.

Including the second integral and other non-ideal gas effects gives slightly modified coefficients:

$$L_{\mathrm{ice}}(T) = 46782.5 + 35.8925T - 0.07414T^2 + 541.5\exp\{-(T/123.75)^2\}, \quad T > 30\ \mathrm{K}, \tag{5}$$

with L_{ice} in J mol^{-1}.

(c) *Extending previous fits*

Following the lead of Jancso *et al.* (1970), we have integrated the Clapeyron equation down in temperature from the triple point. It is possible to substitute Eq. (5) into Eq. (1b) and obtain an analytic result, but the functional form is inconvenient. A better approach is to start by ignoring the last term in Eq. (5). Although this is not highly accurate, it defines a physically based functional form for a later numerical fit. The result is that:

$$\ln(p) = b_0 + b_1/T + b_2\ln(T) + b_3T, \tag{6}$$

where b_0 to b_3 are constants. This functional form was known long ago (Weber 1915), but modern formulae have been more complicated.

In a separate calculation, Eq. (1a) was solved numerically using a fourth order Runge–Kutta solver. This numerical solution included the full Δc_p as well as the terms in both Eqs. (1) and (3) due to the finite volume of ice and non-ideal behaviour of water vapour. The second virial coefficient was taken from Harvey and Lemmon (2004). The form of Eq. (6) was then fitted to the numerical results with a constraint at the triple point. With temperature in K and pressure in Pa the result is:

$$p_{\mathrm{ice}} = \exp(9.550426 - 5723.265/T + 3.53068\ln(T) - 0.00728332T); \quad T > 110\ \mathrm{K}. \tag{7}$$

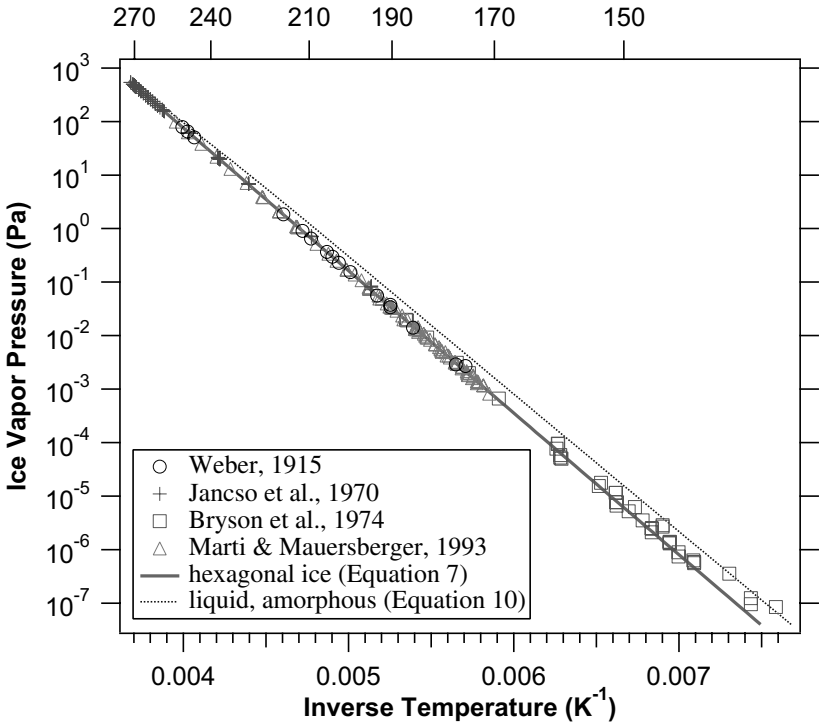

Figure 2. Vapour pressure of ice versus inverse temperature for selected experimental data. The Bryson *et al.* (1974) data below 140 K are probably affected by amorphous ice. Also shown is the vapour pressure of supercooled water.

This fits the numerical solution to within 0.025% from 111 K to the triple point, so the errors in the fitting process are much less than the uncertainties in the thermodynamics. This expression fits the vapour pressure of ice over a wider temperature range with fewer terms than other expressions available in the literature. The good fit also shows that there is no reason to add more terms. Sample values for this and other equations are shown in appendix C.

The frost point, T_{frost}, is defined as that temperature at which the vapour pressure of ice is equal to the ambient water partial pressure p_{w}. Equation (7) cannot be inverted to find T_{frost}. A convenient fit for this, with temperature in K and pressure in Pa, is:

$$T_{\text{frost}} \approx (1.814625\ \ln(p_{\text{w}}) + 6190.134)/(29.120 - \ln(p_{\text{w}})); \quad T > 115\ \text{K}. \quad (8)$$

The residuals for this expression compared to the numerical solution are less than ± 0.04 K above 115 K.

(*d*) *Comparison to vapour pressure data*

Figure 2 shows some of the available data on the vapour pressure of ice along with the results from Eq. (7). When comparing them, one should remember that only one vapour pressure value, that at the triple point, went into Eq. (7). Figure 3 shows a more detailed comparison of some experimental data on the vapour pressure of ice. Although the experimental data confirm the thermodynamic predictions, it is apparent that they do little to narrow the uncertainty compared to integrating the Clapeyron equation. The different experimental techniques show their strengths and weaknesses: Weber (1915)

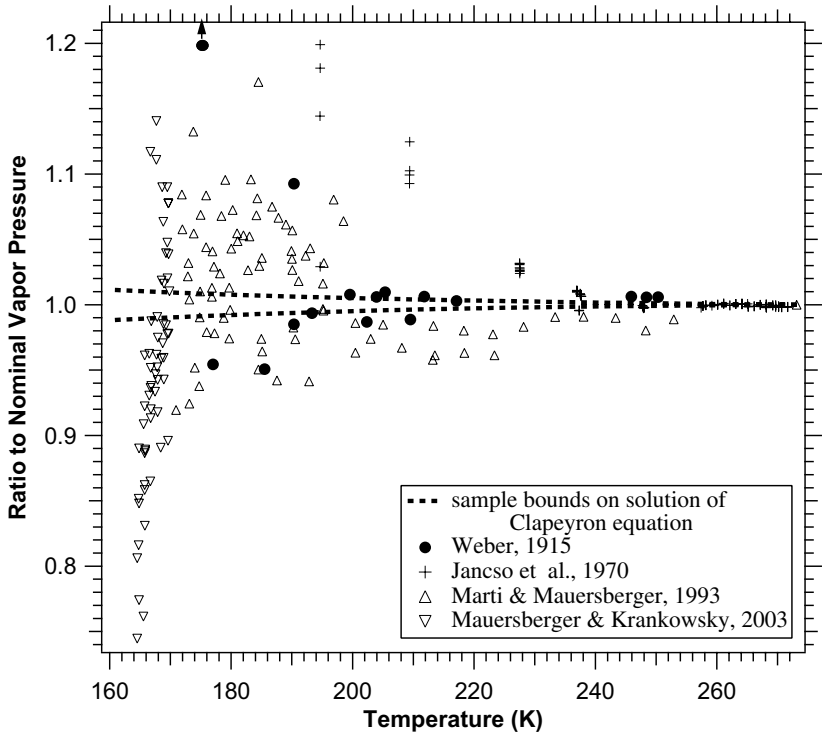

Figure 3. The ratio of selected ice vapour pressure data to that calculated from Eq. (7). One point from Weber (1915) is off-scale at (175, 1.27). The sample bounds consist of changing the latent heat of sublimation of ice at the triple point by ± 20 J mol^{-1}, the molar heat capacity of ice by $\pm 0.5\%$, and the molar heat capacity of water vapour by $\pm 0.3\%$.

and Jancso *et al.* (1970) made direct pressure measurements that are accurate but have limited signal at lower vapour pressures; Marti and Mauersberger (1993) used better vacuum techniques and a mass spectrometer that was very sensitive but required an additional calibration step. Their low vapour pressure data are more reliable than the direct pressure measurements but the higher-temperature data are less accurate.

The experimental vapour pressure data do not imply that any one parametrization of the vapour pressure is best. Equation (7) gives essentially identical results to those of Hyland and Wexler (1983) but with fewer terms (Fig. 4). In addition, Eq. (7) is also applicable over a very wide temperature range. Figure 4 reveals that several parametrizations are within plausible error bounds of each other. The fit used by Marti and Mauersberger (1993) is outside such bounds for much of the temperature range. This is in part because they used the simple form of Eq. (2) to fit data over a wide temperature range. As the temperature range widens the temperature dependence of L_{ice} becomes more important and the form of Eq. (2) is less suitable for fitting.

Practical temperature scales have been revised through the years. Vapour pressure expressions such as Eq. (7), those proposed by Hyland and Wexler (1983) or by Goff (1965) are a combination of experimental data on practical temperature scales which change, and integrations over temperature which do not change. Therefore one cannot simply substitute different temperature scales into the equations. Instead, the experimental data need to be shifted and the equations derived again. This work relies on the Giauque and Stout (1936) specific-heat data. We have shifted their data as best we

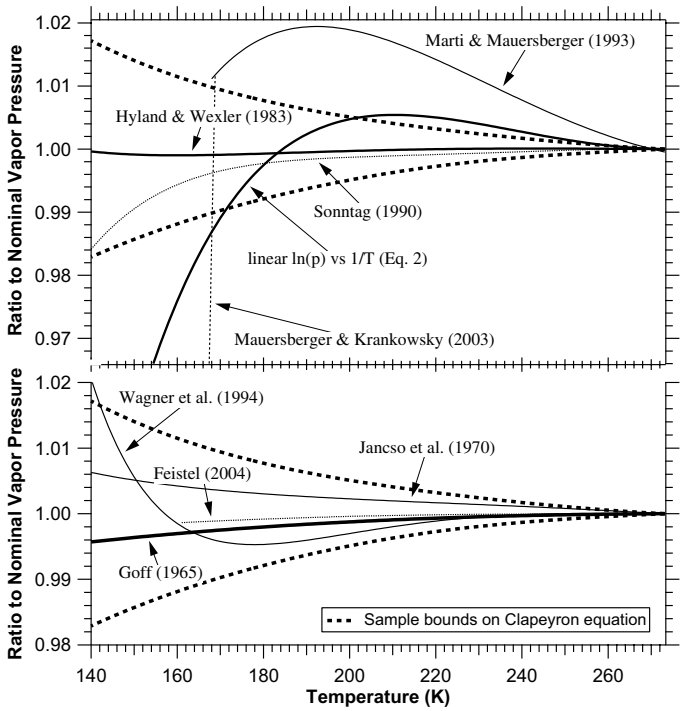

Figure 4. Ratios of various parametrizations of the vapour pressure of ice to the nominal thermodynamic solution expressed here as Eq. (7). The figure is given as two panels to avoid overlap. The Jancso *et al.* (1970) curve is from their Eq. (13).

could to a modern temperature scale but the effect of the shifts on the vapour pressure is very small—less than 0.01% above 160 K. Shifting the Jancso *et al.* (1970) data on Fig. 3 from the 1968 to 1990 temperature scales moves the points by less than half the symbol size at about 200 K, and even less at higher temperatures.

Handbook values for the vapour pressure of ice are not always accurate. The 83rd edition of the CRC tables (Chemical Rubber Company 2002) uses the Wagner *et al.* (1994) parametrization, with minor round-off errors below 200 K. The values in the 55th edition are much less accurate. The Smithsonian Physical Tables (Table 635 in Smithsonian 2003) has errors of up to 3.4%. The Smithsonian Meteorological Tables, 6th edition (Smithsonian 1951) are within about 0.5% of Eq. (7).

Although it does not show up well on Fig. 3, a sharp change in the slope of vapour pressure versus inverse temperature was observed by Mauersberger and Krankowsky (2003). This is reflected in their expression for the vapour pressure (Fig. 4), which quickly goes outside the nominal thermodynamic bounds. One possibility is simply that the slope is not well defined over such a limited temperature range (164.5 to 169 K); alternatively the change in slope might represent a phase change in ice. Because the change is to lower vapour pressures, such a phase would have to be more stable than hexagonal ice. As they note, the implied latent heat at 169 K would be about 7 kJ mol^{-1}. For comparison, 7 kJ mol^{-1} is about half the latent heat of fusion of ice at 0 °C. It is much larger than the entire area of the 'hump' between 50 and 170 K in the molar heat-capacity data (Fig. 1). Therefore, the cause for the change in slope observed by Mauersberger and Krankowsky (2003) is unclear.

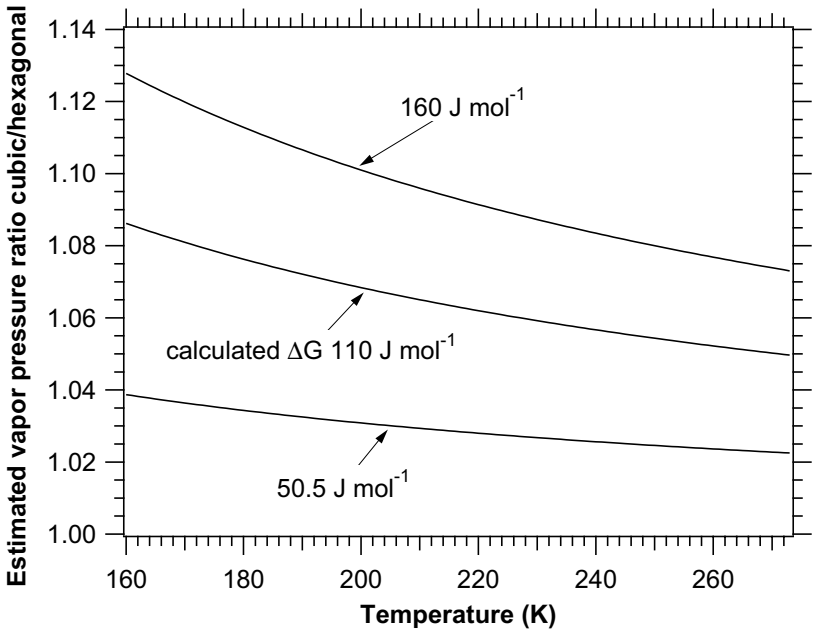

Figure 5. Vapour pressure ratio of cubic to hexagonal ice estimated from measurements of the latent-heat release on transformation of ice from cubic to hexagonal form. This graph assumes that the entropy difference $\Delta S \approx 0$ (Tanaka 1998). Values of the latent heat are 50.5 J mol^{-1} from Handa *et al.* (1986), 56 J mol^{-1} from Mayer and Hallbrucker (1987), 151 J mol^{-1} from McMillan and Los (1965), and 160 J mol^{-1} from Sugisaki *et al.* (1968).

3. METASTABLE ICE

Metastable forms of ice may have affected some of the experimental vapour pressure data below about 200 K. Metastable forms necessarily have a higher vapour pressure than the most stable form, which is hexagonal ice. Most vapour pressure experiments have used ice deposited from the vapour. Besides hexagonal ice, this can also produce cubic and amorphous ice (Hobbs 1974). Below about 200 K cubic ice nucleates first, then transforms to hexagonal ice over a period of minutes to days. This process may influence clouds at the tropical tropopause (Murphy 2003). Below about 160 K amorphous (vitreous) ice can be formed. Some forms of amorphous ice are probably not a well-defined phase since their properties can depend on the deposition rate and temperature (Kouchi 1987).

The vapour pressure of cubic ice does not appear to have been explicitly measured. Cubic ice can be estimated to have a vapour pressure 3 to 11% higher than hexagonal ice at 200 K (Fig. 5). The vapour pressure ratio is just $\exp(\Delta G/RT)$, where $\Delta G = \Delta H - T\Delta S$ is the Gibbs energy difference between hexagonal and cubic ice, and ΔH and ΔS are the corresponding enthalpy and entropy differences. Calculations by Tanaka (1998) indicate that the entropy is nearly identical for cubic and hexagonal ice. If so, then the Gibbs energy difference is equal to the latent heat of transformation between cubic and hexagonal ice, and that is what is shown in Fig. 5. The wide variation in measured ΔH can be attributed to its small magnitude as well as the difficulty in preparing samples of cubic ice that are not contaminated by either amorphous or hexagonal ice. Cubic ice can also be sufficiently disordered to affect its bulk properties (Kohl *et al.* 2000).

The difference in vapour pressures raises the issue of just what vapour pressure some of the low temperature measurements represent. Bryson *et al.* (1974) deposited

their ice at 100 K and do not mention an annealing procedure, so it is likely that their samples were affected by cubic ice, amorphous ice, or both. Indeed, Kouchi (1987) plotted the Bryson *et al.* data as cubic ice. To ensure hexagonal ice, Marti and Mauersberger (1993) annealed their samples for at least 15 minutes at over 200 K. That may not have been quite warm enough to be sure that every sample was completely annealed to hexagonal ice. For example, the calorimeter data of Handa *et al.* (1986) showed that a bulk sample was largely transformed to hexagonal ice in 10 minutes at 200 to 210 K, but complete conversion was not observed until 215 K. Mauersberger and Krankowsky annealed their samples for at least 15 minutes, and usually much longer, at 210 K and verified that the vapour pressure at 210 K was reproducible. To our knowledge, nobody has measured the vapour pressure of ice at low temperatures and confirmed the crystalline structure with electron or x-ray diffraction. There is a need for such measurements, as differences between the vapour pressures of cubic and hexagonal ice might have important implications for high altitude clouds (Murphy 2003).

Another issue that is not yet clear is whether a frost-point hygrometer always measures hexagonal ice at very low temperatures. At times the frost is bluish or nearly clear (Brewer *et al.* 1948). If the ice deposit on a frost-point hygrometer includes other forms of ice than hexagonal, then the frost point will be misleading. The difference between cubic and hexagonal ice is in the right direction to possibly explain some of the persistent differences between frost point and other measurements of water vapour in the stratosphere (Kley *et al.* 2000). Whether or not atmospheric data are affected by cubic ice depends on whether the ice surface is laid down at a high temperature and then maintained under feedback control, or is repeatedly formed and evaporated at the low temperatures.

4. Supercooled water

(*a*) *General remarks*

Supercooled water is metastable with respect to ice, that is, it has a greater Gibbs energy and, hence, a greater vapour pressure than ice. The implications of this vapour pressure difference for mixed clouds were recognized by Wegener at the beginning of the last century and finally led to the theory of precipitating clouds by means of the Bergeron–Findeisen process (Eliassen *et al.* 1978). The earliest experimental studies devoted to determine the vapour pressure of supercooled water date back to 1820 and 1844 (Angell 1982), but the first reliable measurements appear to be those of Scheel and Heuse (1909). More recent studies include those of Bottomley (1978), Kraus and Greer (1984) and Fukuta and Gramada (2003). Such measurements are difficult, since metastable water samples can spontaneously freeze to form ice. Measurements are restricted to temperatures above about 235 K, at which point even very small water droplets freeze homogeneously to ice. This temperature is therefore often termed the homogeneous freezing temperature of water, T_f.

From an atmospheric perspective, there are reasons to be interested in the thermodynamics of supercooled water at temperatures below $T_f \approx 235$ K. By convention relative humidity from radiosonde data is expressed with respect to supercooled water rather than ice (WMO 1988). Water vapour measurements in cirrus clouds have been referenced to the vapour pressure of supercooled water at about 200 K (Heymsfield *et al.* 1998). At a more fundamental level, the vapour pressure of supercooled water is closely related to the water activity of supercooled aqueous solutions. According to its definition, the water activity $a_w = p_{solution}/p_{liq}$, where $p_{solution}$ and p_{liq} are the vapour pressures over a solution and supercooled liquid water, respectively. The water activity is

important for the deliquescence of aerosol particles, the chemical equilibria in aerosols at low temperature (Clegg *et al.* 1998; Wexler and Clegg 2002), and the freezing of supercooled droplets in the atmosphere (Koop *et al.* 2000).

Just as for ice, the Clapeyron equation can be integrated starting from the triple point to calculate the vapour pressure of supercooled water. Because of experimental limitations with supercooled water, there is much greater uncertainty in this calculation. Figure 6 shows three of the more recent measurements of the isobaric molar heat capacity of liquid water (Angell *et al.* 1982; Tombari *et al.* 1999; Archer and Carter 2000). The data stop at ~236 K because it is difficult to supercool water beyond that point. All three datasets, which include both bulk samples and small droplets, show a rapid increase in heat capacity below about 250 K. It is important to note that neither of the two most widely used formulations of the vapour pressure of supercooled water follows the experimental data (Goff 1965; Hyland and Wexler 1983).

In order to extend the heat-capacity data of pure water to lower temperatures, we need to know what happens below T_f. Unfortunately, crystallization of ice can be avoided only by hyperquenching liquid water at extremely high cooling rates exceeding 10^5 K s^{-1} to temperatures below 100 K (Brüggeller and Mayer 1980). This procedure results in an amorphous (vitreous) form of water, often termed amorphous ice. Amorphous ice crystallizes upon warming to about 155 K. Hence, the region between 155 K and 235 K is not accessible to experiments on supercooled water (Mishima and Stanley 1998).

(*b*) *Detailed thermodynamics of supercooled water*

Currently, there are three theories to explain the properties of water in the supercooled temperature range (Mishima and Stanley 1998; Debenedetti 2003). Reviewing them is beyond the scope of this paper, but we present a brief discussion relevant to the work that follows. The first theory is the so-called stability-limit hypothesis (Speedy and Angell 1976; Speedy 1982), which suggests a singularity in various properties of supercooled water (including c_p) at about 228 K. Liquid water cannot exist below this temperature. The second theory, the singularity-free hypothesis, suggests strong changes in thermodynamic properties at about 235 K, but with a thermodynamic continuity between liquid water above and below 235 K (Sastry *et al.* 1996; Rebelo *et al.* 1998). The third suggestion is the liquid–liquid phase transition hypothesis (Poole *et al.* 1992, 1994). It proposes the existence of a second critical point of water at about 220 K and 0.1 GPa (= 1000 bar). It is suggested that this critical point is the cause for the observed strong changes in thermodynamic properties also at ambient pressure.

It is difficult to test experimentally which of these theories is correct. But recent experimental studies and modelling results support some sort of thermodynamic continuity between liquid water above 235 K and amorphous ice at ~155 K. Neutron diffraction measurements show that the structure of liquid water changes towards the amorphous ice structure when cooled at ambient pressure (Bellissent-Funel *et al.* 1992, 1995). Likewise, diffusivity measurements are consistent with the idea that amorphous ice transforms upon warming into a deeply metastable extension of normal liquid water before crystallizing at 160 K (Smith and Kay 1999).

The concept of thermodynamic continuity between liquid water and amorphous ice at normal pressure has an important implication: experimental data on amorphous ice can be used to constrain the thermodynamic functions of water at intermediate (155 K $< T <$ 235 K) temperatures where no data exist (Johari *et al.* 1994; Speedy *et al.* 1996; Bartell 1997; Starr *et al.* 2003). One common conclusion is that the molar heat capacity

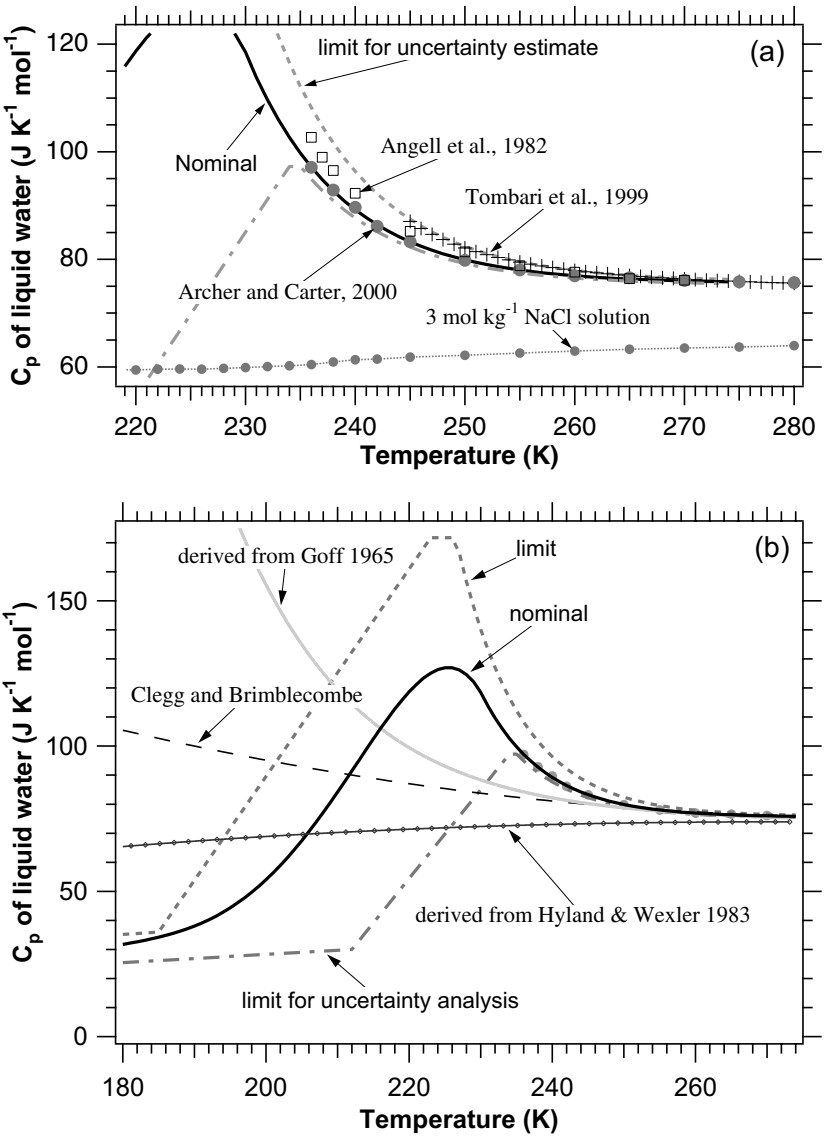

Figure 6. Data and extrapolations for the heat capacity of supercooled water. (a) Experimental data and our nominal fit (thick solid line) and limits (thick dashed curves) used for the uncertainty analysis. The nominal calculation follows Starr *et al.* (2003) but has been slightly modified to match the Archer and Carter (2000) data. Symbols are experimental data from Angell *et al.* (1982), Tombari *et al.* (1999) and Archer and Carter (2000). NaCl solution data from Archer and Carter show how the maximum in molar heat capacity is absent for strong solutions. (b) The nominal fit and limits over a wider temperature range along with values from several literature sources. The Clegg and Brimblecombe (1995) curve is used in the Aerosol Inorganics Model (Wexler and Clegg 2002).

of supercooled water has a maximum just below 235 K, and then decreases until at something like 150 K it is near the heat capacity of ice. Indeed, if the molar heat capacity of supercooled water were to remain above 100 J $K^{-1}mol^{-1}$ then liquid water would be more stable than ice at, say, 100 K. This is unphysical because it implies that hexagonal ice would spontaneously melt to form water upon cooling. As a consequence, the molar heat capacity of water is expected to go through a maximum and to decrease at low temperatures.

Here, we follow these earlier approaches and at the same time include the most recent heat-capacity data by Archer and Carter (2000). Our nominal fit to the molar heat capacity of supercooled water (heavy curve, Fig. 6(a)) starts with an exponential fit to the Archer and Carter (2000) data. This exponential fit together with a value for the latent heat of vaporization of liquid water at the triple point of $L_{\mathrm{liq,t}} = 45051$ J mol^{-1} (Osborne *et al.* 1939; Wagner and Pruss 2002) yields the latent heat of vaporization of supercooled water as:

$$L_{\mathrm{liq}}(T) \approx 56579 - 42.212T + \exp\{0.1149(281.6 - T)\}; \quad 236 \leq T \leq 273.16 \text{ K}. \tag{9}$$

Below 231 K, our nominal fit follows, except for small adjustments, the approach of Starr *et al.* (2003) of estimating the properties of supercooled water within plausible limits. Archer and Carter (2000) argue that the measurements by Angell *et al.* (1982), which were used by Starr *et al.*, were not corrected for the applied cooling rate of 10 K min^{-1}. A correction by 1.8 K brought the two datasets into excellent agreement. Therefore, we have adjusted the upper-temperature portion of the Starr *et al.* (2003) molar heat-capacity curve (derived from a best guess of their excess entropy formulation; F. Starr, personal communication) to match the Archer and Carter (2000) data. Below 167 K the molar heat capacity of water was set to that of hexagonal ice plus 2 J $K^{-1}mol^{-1}$.

The error limits on the vapour pressure of supercooled water are naturally hard to define at temperatures below the molar heat-capacity data. We present two alternative calculations, with and without a constraint based on amorphous ice. Limits without such a constraint are shown as the outer dashed and dash-dotted curves on both Figs. 6(a) and (b). These represent limits on physically plausible behaviour. As described earlier, the molar heat capacity of supercooled water must have a maximum. The two dashed curves represent putting the maximum at the highest temperature allowed by experimental data, or at the lowest temperature allowed without generating unphysical behaviour. Piecewise linear extrapolations were used simply because they are easy to work with.

Alternatively, as discussed above, experimentally determined properties of amorphous ice can be used to constrain the vapour pressure of water. Speedy *et al.* (1996) measured evaporation rates of amorphous and crystalline ice (probably cubic) and derived the ratios shown as squares in Fig. 7. These correspond to a Gibbs energy difference between amorphous and cubic ice of 1100 ± 100 J mol^{-1} at 150 K. The double centre point shows the uncertainty expected depending on whether their crystalline ice was cubic or hexagonal. Johari *et al.* (1994) measured the enthalpy of crystallization of amorphous ice to cubic ice. From this, and estimates of the entropy difference between water and hexagonal ice, they estimated the Gibbs energy difference between amorphous and hexagonal ice to be 1100 ± 300 J mol^{-1} at 153–158 K (circles in Fig. 7). The inner uncertainty limits in Figs. 7 and 8 show alternative calculations of errors that include the same uncertainty in the heat capacity above 235 K as shown on Fig. 6, but are constrained at 150 K to the range of Gibbs energy difference between amorphous and hexagonal ice given by Speedy *et al.* (1996).

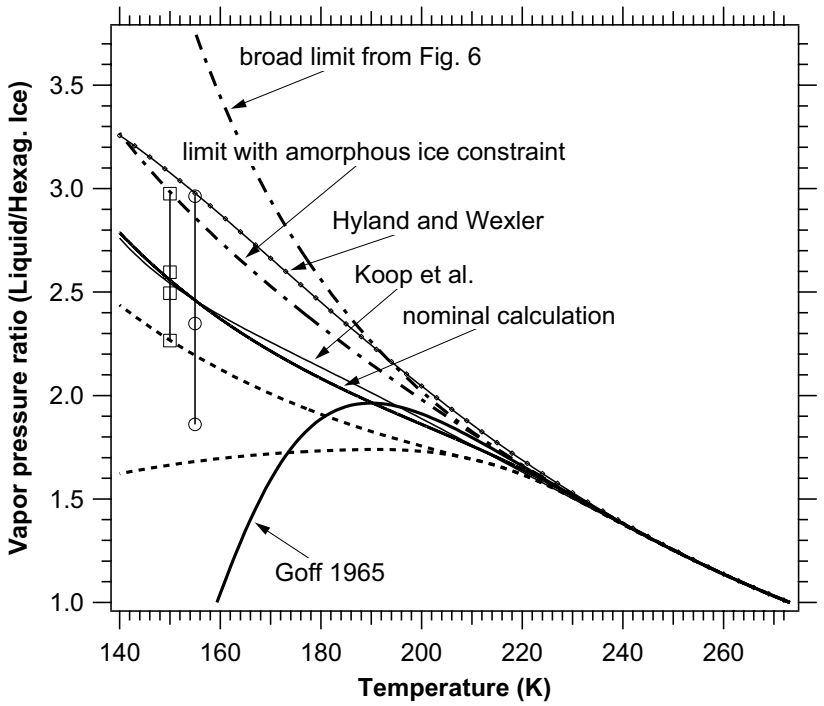

Figure 7. The ratio of the vapour pressure of liquid water to that of hexagonal ice. The vertical bars at 150 and 155 K show estimates of the vapour pressure ratio from Gibbs free energies given in Speedy *et al.* (1996) and Johari *et al.* (1994). Note that the upper limit plotted here corresponds to the lower limit on heat capacity in Fig. 6 and vice versa.

Water vapour data from the atmosphere provide a weak constraint on the vapour pressure of supercooled water. Saturation with respect to ice up to 1.6 or 1.7 has been observed at temperatures of 184 to >210 K (Kelly *et al.* 1993; Heymsfield *et al.* 1998; Haag *et al.* 2003). Assuming the atmosphere does not exceed liquid water saturation by more than about 1%, this means that the uncertainty in the liquid vapour pressure cannot go beyond the lower limit shown on Fig. 6.

Figure 8 compares, on an expanded scale, our nominal case with a number of other parametrizations of the vapour pressure of water. The nominal case here generates vapour pressures at 200 to 240 K that are slightly lower than Goff (1965). This is a consequence of using molar heat-capacity data not available in 1965. Goff's parametrization, and many others, diverge rapidly beyond their intended range of applicability.

The WMO (2000) parametrization, which is based on Goff (1957), should be essentially identical to Goff (1965); instead, a typographical error (see appendix B) leads to a difference of almost 1% at 230 K and rapidly increasing errors below that. The uncorrected formula is outside plausible thermodynamic bounds (Fig. 8). The Hyland and Wexler (1983) parametrization is used for calibration of the widely used Vaisala radiosondes (Miloshevich *et al.* 2001). According to the original paper, the parametrization is only valid above 0 °C (273.15 K). When extrapolated to lower temperatures, the molar heat capacity derived from it using the Clausius–Clapeyron equation is inconsistent with data for supercooled water (Fig. 6). The parametrization is therefore not well suited for use below ~260 K. There is a coincidental correspondence

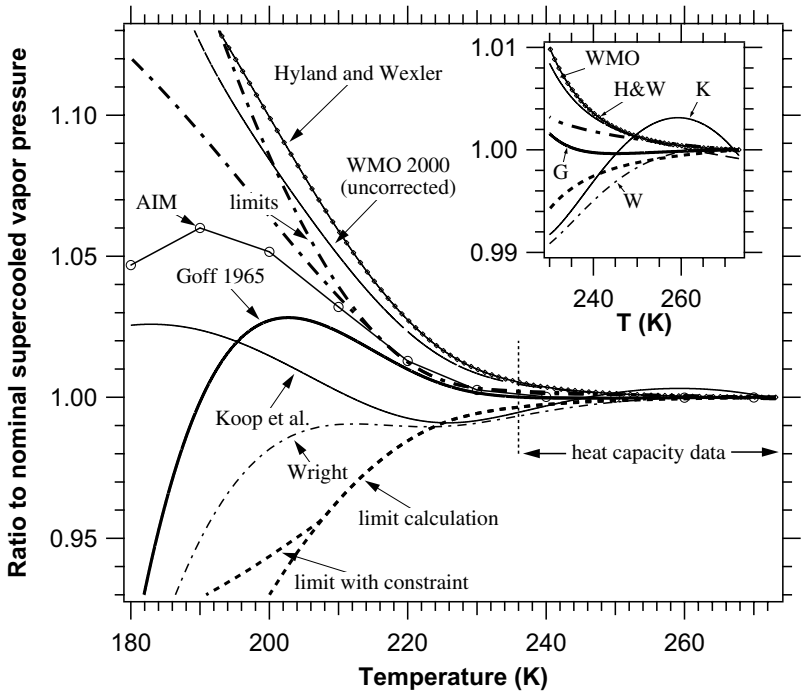

Figure 8. Ratios of parametrizations of the vapour pressure of supercooled water to Eq. (10). The dashed and dash-dotted curves refer to the assumed limits shown in Fig. 6 plus small increments due to changing the latent heat of vaporization at 273.16 K by 20 J mol^{-1}. References are: Goff (1965); Hyland and Wexler (1983); Wright (1997); Clegg *et al.* (1998); Koop *et al.* (2000); Wexler and Clegg (2002). Note that some of the expressions from the literature are plotted here beyond their stated temperature range, simply to illustrate how they would diverge.

between the erroneous WMO (2000) expression and the extrapolated Hyland and Wexler parametrization. This may have misled some into believing that the two agreed with each other.

The maximum in the molar heat capacity of supercooled water makes it difficult to fit its vapour pressure with a simple function. The expression in Koop *et al.* (2000) for the activity of supercooled water (appendix A) is adequate, except that it is not sufficiently accurate near 260 K to express the difference between the vapour pressures of supercooled water and ice. The nominal calculation in this paper was extended upward from the triple point using vapour pressures from Wagner and Pruss (1993). That makes this fit suitable for the entire range of temperatures normally encountered in the atmosphere, not just supercooled water. The fit is:

$$\begin{aligned}\ln(p_{\mathrm{liq}}) \approx\ & 54.842763 - 6763.22/T - 4.210\ln(T) + 0.000367T \\ & + \tanh\{0.0415(T - 218.8)\}(53.878 - 1331.22/T \\ & - 9.44523\ln(T) + 0.014025T);\end{aligned} \tag{10}$$

for $123 < T < 332$ K.

This expression was obtained by first using the form of Eq. (6) to fit separately the calculated vapour pressures on each side of the maximum in molar heat capacity. Then a hyperbolic tangent was used as a continuous and differentiable way of splicing the fits together. It goes to $+1$ for $T \gg 220$ and -1 for $T \ll 220$. Finally, the expression was optimized over the entire temperature range. In the fit, data points from 123 to 233 K were weighted by a factor of $1/8$ to $1/2$ compared to data points at higher temperatures,

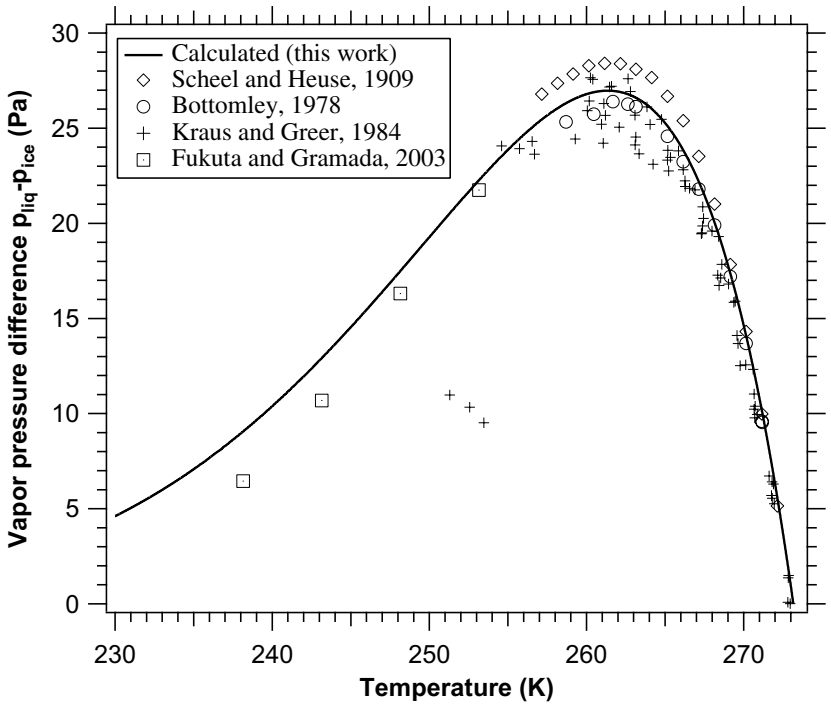

Figure 9. The difference between vapour pressure over water, p_{liq}, and over ice, p_{ice}, according to Eqs. (10) and (7) together with experimental data. The data of Scheel and Heuse (1909) and Bottomley (1978) were used directly. Since Kraus and Greer (1984) and Fukuta and Gramada (2003) provide data on p_{liq}, the vapour pressure difference was calculated using Eq. (7) for p_{ice}. Over this temperature range the uncertainty in the calculation is not much larger than the line width on the graph. The difference between this work and Goff (1965) is similarly small.

because there are no heat-capacity data below 233 K. The residuals compared to the combination of the numerical solution and Wagner and Pruss (1993) are $< 0.05\%$ for $123 < T < 332$ K. The results of Eq. (10) for p_{liq} are shown in Fig. 2 together with the curve for p_{ice}. Interestingly, the lowest temperature data points by Bryson *et al.* (1974) are in agreement with Eq. (10), implying that these measurements do indeed correspond to amorphous ice rather than hexagonal ice.

5. DIFFERENCES BETWEEN p_{liq} AND p_{ice}

The difference between the individual vapour pressures of liquid water and ice is important for applications such as the characteristic time constant for water vapour transfer from liquid water droplets to ice crystals in mixed clouds. Figure 9 shows the difference between the parametrizations for ice and liquid water derived in this work as a function of temperature. Data on the vapour pressure of supercooled water are also shown in Fig. 9 (Scheel and Heuse 1909; Bottomley 1978; Kraus and Greer 1984; Fukata and Gramada 2003). The maximum difference occurs at a temperature of 261.3 K, in accordance with experimental data. Below about 255 K all of the data are lower than the calculation. To explain the Fukata and Gramada (2003) data, the molar heat capacity of water would have to differ from measured values by about a factor of three. This is in a temperature range where the heat capacity of water has been measured by several groups with both small droplets and bulk samples. Therefore, we

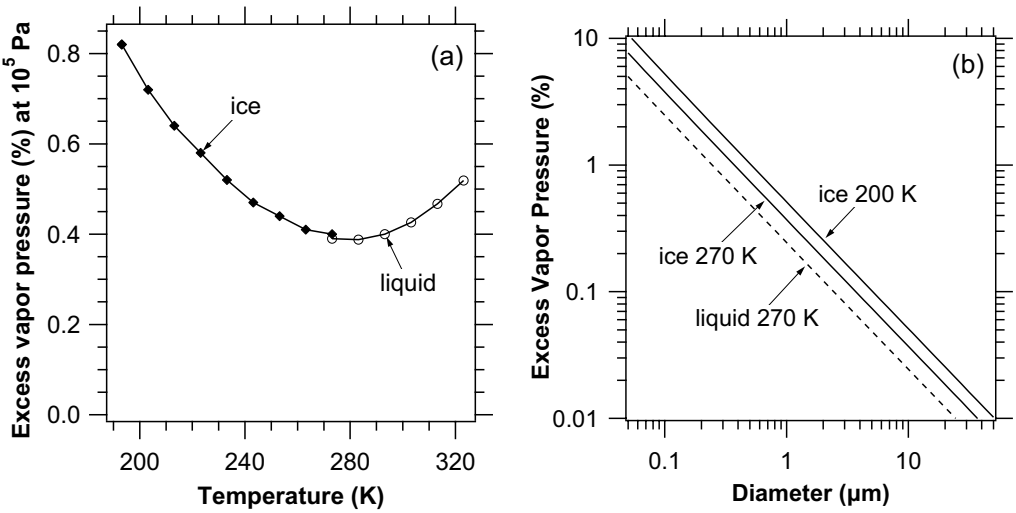

Figure 10. Excess vapour pressure due to: (a) 1000 mb of air (Hyland 1975), and (b) surface energy for spherical particles as a function of diameter, using a surface energy of 0.106 J m^{-2} for ice and 0.076 J m^{-2} for water (Hobbs 1974; Pruppacher and Klett 1997). The excess vapour pressure factor, f, due to atmospheric pressure may be fitted for ice or liquid using: $f = 1 + 10^{-7} p_{\text{air}} (4.923 - 0.0325T + 5.84 \times 10^{-5} T^2)$ for $180 < T < 330$ K and p_{air} in Pa. See text for details.

believe that below 255 K the vapour pressure data must be rejected in favour of the molar heat-capacity data.

6. Other effects on vapour pressure

So far, this discussion has focused on the vapour pressure of bulk samples of pure ice or supercooled water under its own vapour. Other effects need to be considered if very high accuracy is desired.

At a larger total pressure, for example in the presence of air, the vapour pressures of ice or liquid water are increased (Hyland 1975). This comes from the interaction of water vapour with air, and to a lesser extent the compressibility of the condensed phases. At one atmosphere the effect is less than 1%, with a slight temperature dependence (Fig. 10(a)). Below one atmosphere total pressure, the effect may be considered to scale linearly with pressure. For typical atmospheric temperature profiles the result is an increase in vapour pressure by perhaps 0.1% for high altitude clouds to about 0.4% for near-surface clouds.

Very approximately, 0.1% of water in air may be present as monohydrates with oxygen, nitrogen, and other molecules as well as water dimers (Kjaergaard *et al.* 2003). Some of the total air pressure effect may be due to the monohydrates. Going beyond the 0.1% accuracy level in measuring water vapour will require an understanding of how a given technique responds to hydrates and dimers. For example, an optical absorption line might not measure dimers.

Solutes can have a large effect on the vapour pressure of water. Pruppacher and Klett (1997) present an extensive discussion of this. The effect of solutes is strongly temperature dependent for supercooled solutions (Archer and Carter 2000). For activation of most aerosol particles into cloud droplets, however, the particles are sufficiently dilute that the properties are close to those of pure supercooled water. The effects of solutes on ice are difficult to ascertain because of the wide range of possible solutes,

as well as non-equilibrium amounts of dissolved material left in the ice when rapidly frozen water is unable to expel all of a solute (Hobbs 1974). However, the effect on the vapour pressure is probably fairly small for atmospheric applications. Coatings, such as organic films, can change the accommodation coefficient of water vapour on ice and otherwise change the approach to equilibrium. However, only changes in the bulk phase of the ice change the basic vapour pressure.

Precipitation changes the isotopic composition of water in the upper atmosphere. However, water is about 99.7% $H_2^{16}O$, so changes in the overall vapour pressure caused by isotopic fractionation will be very small.

Because of surface energy, small ice crystals and water droplets only a few micrometers in diameter have vapour pressures that are larger than those of bulk phases by a fraction of a percent. Figure 10(b) shows this excess vapour pressure resulting from surface energy (Pruppacher and Klett 1997). Various coatings and adsorbed species may modulate this surface energy effect. Gao *et al.* (2004) suggested an association with adsorbed HNO_3 as the cause of an observed supersaturation in clouds below 200 K. The supersaturation with respect to hexagonal ice was 10 to 30%, depending on whether or not one scales the water vapour data above 200 K to the ice vapour pressure. For a surface layer to change the vapour pressure of ice crystals larger than about 1 μm by 10%, the surface energy would have to increase by a factor of about 100. Alternatively, the reason for the supersaturation could be cubic ice, failure to reach equilibrium, or even other mechanisms.

A final consideration for highly accurate atmospheric water vapour measurements comes from the nonlinear dependence of the vapour pressure on temperature. For example, for normally distributed temperature values with a standard deviation of 1 K, the vapour pressure at the average temperature differs from the true average vapour pressure by 0.4% at 255 K or 1% at 200 K. Using data from a long horizontal transect in the upper troposphere (Tuck *et al.* 2004), 200 km averages of the temperature would have led to errors of 0.1 to 1.4% in the average vapour pressure of ice. Therefore, more accurate relative-humidity data would require not only better measurements of both temperature and water vapour but also better spatial and temporal resolution in those measurements.

7. Water activity, deliquescence and homogeneous ice nucleation

Upon cooling, aerosol particles take up water from the gas phase in order to maintain equilibrium between the water vapour pressure of the aerosol particles, p_{solution}, and the gas-phase water partial pressure, p_{w}. Deliquescence and subsequent ice nucleation may occur during this simultaneous cooling and dilution. Calculations can be performed with the help of the following equalities:

$$a_{\text{w}} \equiv \frac{p_{\text{solution}}}{p_{\text{liq}}} \overset{\text{at equilibrium}}{=} \frac{p_{\text{w}}}{p_{\text{liq}}} \equiv RH_{\text{liq}} = RH_{\text{ice}} \frac{p_{\text{ice}}}{p_{\text{liq}}}. \tag{11}$$

According to its definition, the water activity a_{w} is equal to the ratio $p_{\text{solution}}/p_{\text{liq}}$. If the aerosol droplets are in thermodynamic equilibrium with the surrounding air, p_{solution} is equal to p_{w}. Hence, under equilibrium conditions we can calculate a_{w} directly from p_{w} and the temperature dependent expression for p_{liq}. It is interesting to note that under equilibrium conditions a_{w} in the droplets is equal to the gas-phase relative humidity with respect to liquid water, RH_{liq}.

Data on deliquescence and freezing behaviour are sometimes limited by the accuracy with which the vapour pressure of supercooled water is known (e.g. Cziczo and

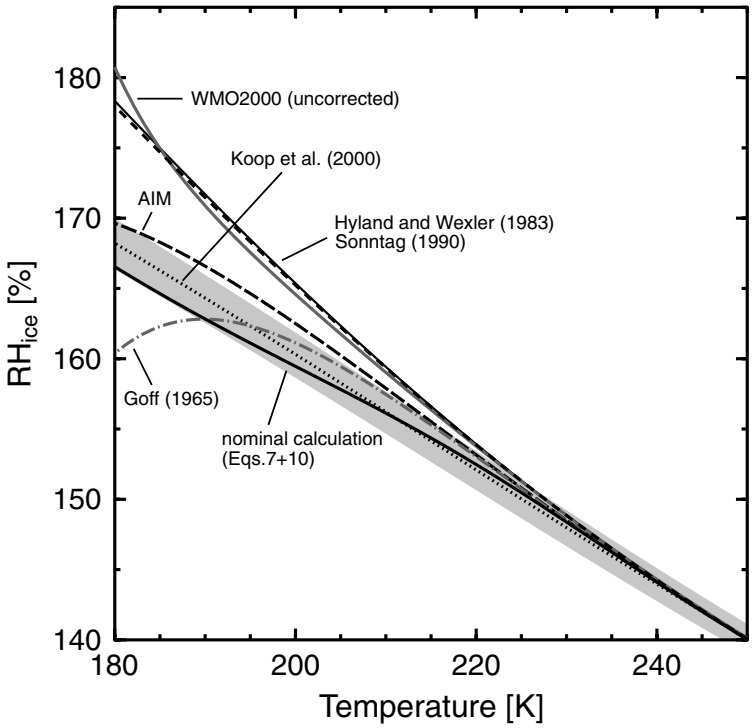

Figure 11. Relative humidity with respect to ice, $RH_{\rm ice}$, for liquid aerosol droplets that are in equilibrium with the surrounding water partial pressure and a homogeneous ice nucleation rate coefficient of $J = 10^{13}$ cm^{-3}s^{-1} as calculated using Eq. (11). Various expressions for the vapour pressure over water and over ice were used. The grey area indicates the values that correspond to varying J between 10^{11} and 10^{15} cm^{-3}s^{-1} (Koop *et al.* 2000). References are as in Fig. 8.

Abbatt 2001; Parsons *et al.* 2004). For example, field measurements of the freezing behaviour of ambient aerosols showed nearly a step-function change from 0.03% to 30% of the particles freezing when the relative humidity was varied from 99% to 101% with respect to liquid water at roughly 223 K (DeMott *et al.* 2003). In this case, the uncertainty in the vapour pressure exceeds the precision of the ambient data. Because of the large uncertainty in the vapour pressure it is important that such papers clearly state which parametrization was used.

Homogeneous ice nucleation in liquid aerosol particles can be calculated with a water-activity-based theory (Koop *et al.* 2000). Figure 11 shows the results of using different expressions for $p_{\rm ice}$ and $p_{\rm liq}$ to calculate the aerosol droplet water activity that corresponds to a homogeneous nucleation rate coefficient of $J = 10^{13}$ cm^{-3}s^{-1}. This rate implies a median freezing time of 1 s for aerosol droplets with a diameter of 0.5 μm. The resulting $a_{\rm w}$ values at different temperatures were used in Eq. (11) to get the corresponding $RH_{\rm ice}$ values together with various expressions for $p_{\rm liq}$ and $p_{\rm ice}$. While the results shown in Fig. 11 are simplified, because the equilibrium between the gas and liquid phase is not always maintained in the atmosphere (for example in strong updraughts), they do provide insight into the effects of using different water vapour parametrizations on the predicted ice nucleation conditions.

The use of the various parametrizations yields differences of up to 20% $RH_{\rm ice}$ at the lowest temperatures. The highest values are found for the expressions of Sonntag (1990),

Hyland and Wexler (1983) and the uncorrected expression from WMO (2000), while the formulation of Goff (1965) yields the lowest RH_{ice} values. The results from the AIM model (Wexler and Clegg 2002), the expression of Koop *et al.* (2000), and the nominal case presented as Eqs. (7) and (10) in this paper are all very close to each other, within the uncertainty of the nucleation model. Therefore, we recommend using any of the latter three formulations for p_{liq} and p_{ice} to predict ice nucleation conditions that are in accordance with the derivation of water-activity-based ice nucleation theory (Koop *et al.* 2000). Note that ice nucleation rates are very sensitive to small changes in RH_{ice}, as indicated by the grey shaded area in Fig. 11 which denotes nucleation coefficient values varying between $J = 10^{11}$ and 10^{15} cm^{-3}s^{-1}, i.e. over four orders of magnitude.

8. Conclusions and future needs

There is basic agreement between the measurements of the vapour pressure of ice and the thermodynamic parametrizations derived from the Clapeyron equation (Fig. 3). All of the commonly used expressions for the vapour pressure of ice, except that of Marti and Mauersberger (1993), are within 1% of each other for temperatures between 170 and 273 K. The experimental vapour pressure data do not select any of the remaining expressions as superior. Equations (7) and (8), derived above, give the vapour pressure of ice and the frost point with fewer terms than other expressions in the modern literature and over a wider temperature range.

The uncertainty in the vapour pressure of ice is not large enough to explain the differences between frost point and other measurements of water vapour pressure in the stratosphere. For many atmospheric applications, the uncertainty in the vapour pressure of ice is small compared to other uncertainties. For example, there is a range exceeding a factor of ten in estimates of the uptake coefficient of water vapour on ice at 200 K (Chaix *et al.* 1998). This uncertainty propagates into computer models of cirrus clouds (Lin *et al.* 2002; Gierens *et al.* 2003). For most atmospheric questions involving ice, the accommodation coefficient is a more important open issue than the vapour pressure.

It is impressive to consider the quality of the vapour pressure data of Weber (1915). He read a mercury manometer with a microscope to a precision of 3 μm for both direct measurements and calibration of a hot-wire probe. At pressures high enough so that he was not limited by vacuum pumping, his data lie within 1% of modern results even though the temperature-scale was defined differently in 1915.

To move to the next ($\sim$0.1%) level of accuracy in the vapour pressure of ice, new data will be required not only on the thermodynamics of bulk ice but also on trapped solutes, surface energy and the stabilization of water vapour by air. Future data on the vapour pressure or latent heat of ice below 200 K should include a measurement of the crystal structure. The heat of fusion of water at the triple point is also a candidate for a new measurement: the standard reference (Osborne 1939) is actually a recalculation from data obtained before 1914. Many fundamental units have been redefined since then.

For liquid water there is good agreement between the Clapeyron equation and measurements of the vapour pressure down to about 255 K. Below that, the vapour pressure measurements are low, as if they had been influenced by the presence of ice. The vapour pressure of liquid water is quite uncertain below about 230 K because the molar heat capacity of liquid water can only be measured until samples freeze at about 236 K. The uncertainty in p_{liq} at 200 K is larger than $\pm$5% and increases rapidly below that. The uncertainty in the vapour pressure at low temperatures is smaller if the properties of supercooled water are related to amorphous ice. Given the large uncertainty

in the vapour pressure of supercooled water, it may be more appropriate to report RH_{ice} below the freezing temperature rather than the meteorological convention of always using RH_{liq}.

Widely used expressions for water vapour (Goff and Gratch 1946; Hyland and Wexler 1983) are being applied outside the ranges of data used by the original authors for their fits. This work may be the first time that data on the molar heat capacity of supercooled water have been used to constrain its vapour pressure.

The most important open issue involving supercooled water is whether thermodynamic data of any kind can be obtained at temperatures well below 230 K, perhaps by using high pressures or nano-droplets and very fast experiments (Bartell 1997). Resolving the theoretical question of the relation between amorphous ice and highly supercooled water would also help define the uncertainty in the vapour pressure.

Acknowledgements

Many people have contributed to this work. We thank, among others: D. Archer for computer code on the properties of NaCl solutions; R. Feistel for a pre-publication version of his ice thermodynamic model; R. Gao for discussions that helped prompt this work; S. Hovde for checking some of the equations; F. Starr for providing his excess entropy formulation; H. Vömel for references; and S. Clegg, A. Harvey, B. Luo, L. Miloshevich and A. S. Wexler for helpful comments and discussion.

Appendix A

Vapour pressure parametrizations and stated range of validity

Here, T_t is the triple point 273.16 K, log is the logarithm to base 10, and ln is the natural logarithm. For parametrizations from this work see Eqs. (7) and (10). A variety of other equations are listed and graphed at http://cires.colorado.edu/~voemel/vp.html (last accessed 12 January 2005). The computational speed of 25 equations was tested by Gueymard (1993).

Goff and Gratch (1946): Units are converted here from atmospheres to Pa. Stated ranges: $184 < T < 273.16$ K for ice and $273.15 < T < 373.15$ K for liquid.

$$\begin{aligned}\log(p_{ice}) = &-9.09718\{(273.16/T) - 1\} - 3.56654\log(273.16/T)\\ &+ 0.876793\{1 - (T/273.16)\} + \log(610.71).\\ \log(p_{liq}) = &-7.90298\{(373.16/T) - 1\} + 5.02808\log(373.16/T)\\ &- 1.3816 \cdot 10^{-7}(10^{11.344(1-T/373.16)} - 1)\\ &+ 8.1328 \cdot 10^{-3}(10^{-3.49149(373.16/T-1)} - 1) + \log(101325).\end{aligned}$$

Goff (1957): Units are converted here from atmospheres to Pa. Stated ranges $180 < T < 273.16$ K for ice and $273.15 < T < 373.15$ K for liquid with extension to 223 K.

$$\begin{aligned}\log(p_{ice}) = &\log(611.14) - 9.096853(T_t/T - 1) - 3.566506\log(T_t/T)\\ &+ 0.876812(1 - T/T_t).\\ \log(p_{liq}) = &\log(611.14) + 10.79574(1 - T_t/T) - 5.0280\log(T/T_t)\\ &+ 1.50475 \cdot 10^{-4}(1 - 10^{-8.2969(T/T_t-1)})\\ &+ 0.42873 \cdot 10^{-3}(10^{4.76955(1-T_t/T)} - 1).\end{aligned}$$

Goff (1965): Units are converted here from atmospheres to Pa. The range is the same as Goff (1957). This 1965 publication, taken from the proceedings of a conference in 1963, has also been frequently referenced as Goff 1963. It is a minor correction to Goff (1957).

$$\begin{aligned}\log(p_{\text{ice}}) &= \log(611.11) - 9.096936(T_{\text{t}}/T - 1) - 3.56654\log(T_{\text{t}}/T)\\ &\quad + 0.876817(1 - T/T_{\text{t}}).\\ \log(p_{\text{liq}}) &= \log(611.11) + 10.79586(1 - T_{\text{t}}/T) - 5.02808\log(T/T_{\text{t}})\\ &\quad + 1.50474\cdot 10^{-4}(1 - 10^{-8.29692(T/T_{\text{t}}-1)})\\ &\quad + 0.42873\cdot 10^{-3}(10^{4.76955(1-T_{\text{t}}/T)} - 1).\end{aligned}$$

Hyland and Wexler (1983), also in Wexler and Hyland (1983): Stated ranges $173.16 \le T < 273.16$ for ice and $273.15 \le T \le 473.15$ for liquid.

$$\begin{aligned}\ln(p_{\text{ice}}) &= (-5674.5359/T + 6.3925247 - 0.96778430\cdot 10^{-2}T\\ &\quad + 0.62215701\cdot 10^{-6}T^2 + 0.20747825\cdot 10^{-8}T^3\\ &\quad - 0.94840240\cdot 10^{-12}T^4 + 4.1635019\ln T).\\ \ln(p_{\text{liq}}) &= (-5800.2206/T + 1.3914993 - 0.48640239\cdot 10^{-1}T\\ &\quad + 0.41764768\cdot 10^{-4}T^2 - 0.14452093\cdot 10^{-7}T^3 + 6.5459673\ln(T)).\end{aligned}$$

Jancso *et al.* (1970) data fit: $\sim 195 < T < 273.16$ K:

$$\begin{aligned}\log(p'_{\text{ice}}) &= -2668.726/T + 10.43112, \text{ (torr)}.\\ p_{\text{ice}} &= 133.32(611.657/611.283)\,p'_{\text{ice}};\\ &\quad \text{corrects for units and triple-point pressure.}\end{aligned}$$

Jancso *et al.* (1970) thermodynamic derivation: $\sim 173 < T < 273.16$ K:

$$\begin{aligned}\log(p'_{\text{ice}}) &= -2481.604/T + 3.5721988\log T - 3.097203\cdot 10^{-3}T\\ &\quad - 1.7649\cdot 10^{-7}T^2 + 1.901973.\\ p_{\text{ice}} &= 133.32(611.657/611.283)\,p'_{\text{ice}};\\ &\quad \text{corrects for units and triple-point pressure.}\end{aligned}$$

Koop *et al.* (2000): $150 < T < 273$ K:

$$\begin{aligned}p_{\text{liq}} \approx p_{\text{ice}}\exp(&-(210368 + 131.438T - 3.32373\cdot 10^{6}/T\\ &- 41729.1\ln(T))/RT).\end{aligned}$$

Marti and Mauersberger (1993): $169 < T < 273.16$ K:

$$p_{\text{ice}} = \exp(28.868 - 6132.9/T).$$

Mauersberger and Krankowsky (2003): $164.5 < T < 169$ K:

$$p_{\text{ice}} = \exp(34.262 - 7044/T).$$

Sonntag (1990): Stated ranges are $173.15 \le T \le 273.16$ K for ice and $173.15 \le T \le 373.15$ K for liquid, despite being based on Wexler (1976).

$$\begin{aligned}p_{\text{ice}} &= 100\exp(24.7219 - 6024.5282/T + 1.0613868\cdot 10^{-2}T\\ &\quad - 1.3198825\cdot 10^{-5}T^2 - 0.49382577\ln(T)).\\ p_{\text{liq}} &= \exp(16.635764 - 6096.9385/T - 2.711193\cdot 10^{-2}T\\ &\quad + 1.673952\cdot 10^{-5}T^2 + 2.433502\ln(T)).\end{aligned}$$

Wright (1997), US Meteorological Handbook:

$$p_{\mathrm{liq}} = 611.21 \exp\{17.502(T - 273.15)/(240.97 + T - 273.15)\}.$$

Wagner and Pruss (1993): $273.16 \le T \le 647$ K:

$$\ln\{p_{\mathrm{liq}}/(2.2064 \cdot 10^7)\} = (T_{\mathrm{c}}/T)(-7.85951783\tau + 1.84408259\tau^{1.5} - 11.7866497\tau^3 + 22.6807411\tau^{3.5} - 15.9618719\tau^4 + 1.80122502\tau^{7.5}),$$

where $\tau = 1 - T/T_{\mathrm{c}}$ and $T_{\mathrm{c}} = 647.096$ K.

Wagner *et al.* (1994): $190 < T < 273.16$ K:

$$\ln p_{\mathrm{ice}} = \ln(611.657) - 13.9281690(1 - (T_{\mathrm{t}}/T)^{1.5}) + 34.7078238(1 - (T_{\mathrm{t}}/T)^{1.25}).$$

Wexler (1976): 0 to 100 °C: $\ln p_{\mathrm{liq}} = \sum_{i=0}^{6} g_{\mathrm{i}} T^{i-2} + g_7 \ln T$, where T is on the IPTS-68 scale* and

$$g_{\mathrm{i}} = \{-0.29912729 \cdot 10^4 - 0.60170128 \cdot 10^4 + 0.1887643854 \cdot 10^2 - 0.28354721 \cdot 10^{-1} + 0.17838301 \cdot 10^{-4} - 0.84150417 \cdot 10^{-9} + 0.44412543 \cdot 10^{-12} + 0.2858487 \cdot 10^1\}.$$

APPENDIX B

Typographical errors in the literature

In the course of preparing this review, we uncovered a number of typographical errors in the literature. No doubt there are additional errors awaiting discovery.

Archer and Carter (2000): In their equation (A.1), the coefficients a_{i} should be outside the braces (D. Archer, personal communication, 2004).

Jancso *et al.* (1970): The value at −3.471 °C in their Table 1 is incorrect.

McDonald (1965): Although the equation given for the vapour pressure of supercooled water is correct, the tabulated values contain systematic errors that reach about 50% at −100 °C. Figure 1 is in error by a similar amount.

Pruppacher and Klett (1997). In the second edition, Eq. (5.12) for the surface tension of water matches their corresponding figure only when $T \le 0$ °C.

Smithsonian Physical Tables (Smithsonian 2003): Table 635 for the vapour pressure of ice contains numerous errors, most notably the points at −67, −59, −52, and −25 °C. This does not apply to the Smithsonian Meteorological Tables (Smithsonian 1951) which are derived from a different formula.

Tombari *et al.* (1999): Their equation in the caption to their Fig. 1 should contain 0.044 rather than 0.44 (E. Tombari, personal communication, 2002).

WMO (1988, 2000): In Eq. (13) of appendix A in the 1988 version the log term on the first line has the wrong sign; there is a misplaced T in the exponent of 10 on the second line; and the sign of the power of 10 on the third line should be positive. The correct expression is from Goff (1957; see our appendix A). In the WMO 2000 corrigendum the first two errors are corrected but the third one remains. The error is about 1% at 230 K and increases rapidly below that.

* International Practical Temperature Scale of 1968.

APPENDIX C

Selected values

TABLE C1. VALUES RECOMMENDED FOR CHECKING COMPUTER CODES

Temperature (K)	Ice vapour pressure[a] (Pa)	Liquid vapour pressure[a] (Pa)	Ice molar heat capacity ($J\ mol^{-1}K^{-1}$)	Liquid molar heat capacity[b] ($J\ mol^{-1}K^{-1}$)	Ice latent heat ($J\ mol^{-1}$)	Liquid latent heat[b] ($J\ mol^{-1}$)
150	$6.106 \cdot 10^{-6}$	$1.562 \cdot 10^{-5}$	22.10	*24.10*	50623	*49119*
180	0.0053975	0.011239	25.70	*31.75*	50906	*49314*
210	0.70202	1.2335	29.47	*84.22*	51081	*48841*
240	27.272	37.667	33.46	89.22	51139	46567
273.15	611.154	611.213	38.09	75.86	51059	45051
273.16	611.657	611.657	38.09	75.85	51059	45051
300	–	3536.8	–	(c)	–	(c)

[a]These values are calculated using double precision; Eqs. (7) and (10) give acceptable results using single precision, although the last digits may vary.

[b]Italics represent values used in this paper but beyond the range of Eq. (9). A polynomial was used for c_p for $167 < T < 231$ K with coefficients (38565.2, −635.6299, 0.964911, 0.03646245, −0.0002189861, $4.197441 \cdot 10^{-8}$, $2.456321 \cdot 10^{-9}$, $-4.839049 \cdot 10^{-12}$).

[c]Water vapour pressures above the triple point were fitted to Wagner and Pruss (1993), so the molar heat capacities and latent heats are approximately as defined in that paper.

REFERENCES

Angell, C. A. 1982 Supercooled water. Pp. 1–81 in *Water: A comprehensive treatise*. Volume 7. Ed. F. Franks. Plenum Press, New York, USA

Angell, C. A., Oguni, M. and Sichina, W. J. 1982 Heat capacity of water at extremes of supercooling and superheating. *J. Phys. Chem.*, **86,** 998–1002

Archer, D. G. and Carter, R. W. 2000 Thermodynamic properties of the NaCl + H_2O system. 4: Heat capacities of H2O and NaCl(aq) in cold-stable and supercooled states. *J. Phys. Chem.*, **104,** 8563–8584

Bartell, L. S. 1997 On possible interpretations of the anomalous properties of supercooled water. *J. Phys. Chem. B*, **101,** 7573–7583

Bellissent-Funel, M. C. and Bosio, L. 1995 A neutron scattering study of liquid D_2O. *J. Chem. Phys.*, **102,** 3727–3735

Bellissent-Funel, M. C., Bosio, L., Hallbrucker, A., Mayer, E. and Sridi-Dorbez, R. 1992 X-ray and neutron scattering studies of the structure of hyperquenched glassy water. *J. Chem. Phys.*, **97,** 1282–1286

Bottomley, G. A. 1978 The vapour pressure of supercooled water and heavy water. *Aust. J. Chem.*, **31,** 1177–1180

Brewer, A. W., Cwilong, B. and Dobson, G. M. B. 1948 Measurement of absolute humidity in extremely dry air. *Proc. Phys. Soc.*, **60,** 52–70

Brüggeller, P. and Mayer, E. 1980 Complete vitrification in pure liquid water and dilute aqueous solutions. *Nature*, **288,** 569–571

Bryson, C. E. III, Cazcarra, V. and Levenson, L. L. 1974 Sublimation rates and vapor pressures of H_2O, CO_2, N_2O and Xe. *J. Chem. Eng. Ref. Data*, **19,** 107–110

Buck, A. L. 1981 New equations for computing vapor pressure and enhancement factor. *J. Appl. Meteorol.*, **20,** 1527–1532

Chaix, L., van den Bergh, H. and Rossi, M. J. 1998 Real-time kinetic measurements of the condensation and evaporation of D_2O molecules on ice at 140 K < T < 220 K. *J. Phys. Chem. A*, **102,** 10300–10309

Chemical Rubber Company 2002 *Handbook of chemistry and physics*. Eighty-third edition. CRC Press, Cleveland, USA

Clegg, S. L. and Brimblecombe, P. 1995 Application of a multicomponent thermodynamic model to activities and thermal properties of 0–40 mol kg^{-1} aqueous sulfuric acid from <200 to 328 K. *J. Chem. Eng. Ref. Data*, **40,** 43–64

Clegg, S. L., Brimblecombe, P. and Wexler, A. S. 1998 Thermodynamic model of the system H^+–NH_4^+–SO_4^{2-}–NO_3^-–H_2O at tropospheric temperatures. *J. Phys. Chem. A*, **102,** 2137–2154

Cziczo, D. J. and Abbatt, J. P. D. 2001 Ice nucleation in NH_4HSO_4, NH_4HO_3, and H_2SO_4 aqueous particles: Implications for cirrus cloud formation. *Geophys. Res. Lett.*, **28,** 963–966

Debenedetti, P. G. 2003 Supercooled and glassy water. *J. Phys. Condens. Matter*, **15,** R1669–R1726

DeMott, P. J., Cziczo, D. J., Prenni, A. J., Murphy, D. M., Kreidenweis, S. M., Thomson, D. S. and Borys, R. 2003 Measurements of the concentration and composition of nuclei for cirrus formation. *Proc. Natl. Acad. Sci.*, **100,** 14655–14660

Eliassen, A., Blanchard, D. C. and Bergeron, T. 1978 The life and science of Tor Bergeron. *Bull. Am. Meteorol. Soc.*, **59,** 387–392

Feistel, R. and Wagner, W. 2005 High-pressure thermodynamic Gibbs functions of ice and sea ice. *J. Mar. Res.*, in press

Flubacher, P., Leadbetter, A. J. and Morrison, J. A. 1960 Heat capacity of ice at low temperatures. *J. Chem. Phys.*, **33,** 1751–1755

Friedman, A. S. and Haar, L. 1954 High-speed machine computation of ideal thermodynamic functions I. Isotopic water molecules. *J. Chem. Phys.*, **22,** 2051–2058

Fukuta, N. and Gramada, C. M. 2003 Vapor pressure measurement of supercooled water. *J. Atmos. Sci.*, **60,** 1871–1875

Gao, R. S., Popp, P. J., Fahey, D. W., Marcy, T. P., Herman, R. L., Weinstock, E. M., Baumgardner, D. G., Garrett, T. J., Rosenlof, K. H., Thompson, T. L., Bui, P. T., Ridley, B. A., Wofsy, S. C., Toon, O. B., Tolbert, M. A., Kärcher, B., Peter, Th., Hudson, P. K., Weinheimer, A. J. and Heymsfield, A. J. 2004 Evidence that nitric acid increases relative humidity in low-temperature cirrus clouds. *Science*, **303,** 516–520

Giauque, W. F. and Stout, J. W. 1936 The heat capacity of ice from 15 to 273 K. *J. Am. Chem. Soc.*, **58,** 1144–1140

Gierens, K. M., Monier, M. and Gayet, J. F. 2003 The deposition coefficient and its role for cirrus clouds. *J. Geophys. Res.*, **108**(D2)**,** Art. No. 4069

Goff, J. A. 1957 Saturation pressure of water on the new Kelvin scale. *Trans. Am. Soc. Heating Air-Cond. Eng.*, **63,** 347–354

1965 Saturation pressure of water on the new Kelvin scale. In *Humidity and moisture: Measurement and control in science and industry*. Volume 3. Ed. A. Wexler. Reinhold Publishing, New York, USA

Goff, J. A. and Gratch, S. 1946 Low-pressure properties of water from −160 to 212 F. *Trans. Am. Soc. Heating Air-Cond. Eng.*, **52,** 95–122 (presented at the 52nd annual meeting of the American society of heating and ventilating engineers, New York)

Gueymard, C. 1993 Assessment of the accuracy and computing speed of simplified saturation vapor equations using a new reference dataset. *J. Appl. Meteorol.*, **32,** 1294–1300

Guildner, L. A., Johnson, D. P. and Jones, F. E. 1976 Vapor pressure of water at its triple point. *J. Res. Natl. Bur. Stand.*, **80A,** 505–521

Haag, W., Kärcher, B., Ström, J., Minikin, A., Lohmann, U., Ovarlez, J. and Stohl, A. 2003 Freezing thresholds and cirrus cloud formation mechanisms inferred from *in situ* measurements of relative humidity. *Atmos. Chem. Phys. Discuss.*, **3,** 3267–3299

Handa, Y. P., Klug, D. D. and Whalley, E. 1986 Difference in energy between cubic and hexagonal ice. *J. Phys. Chem.*, **84,** 7009–7010

Harvey, A. H. and Lemmon, E. W. 2004 Correlation for the second virial coefficient of water. *J. Phys. Chem. Ref. Data*, **33,** 369–376

Heymsfield, A. J., Miloshevich, L. M., Twohy, C., Sachse, G. and Oltmans, S. 1998 Upper-tropospheric relative humidity observations and implications for cirrus ice nucleation. *Geophys. Res. Lett.*, **25,** 1343–1346

Hobbs, P. V. 1974 *Ice physics*. Clarendon Press, Oxford, UK

Hyland, R. W. 1975 A correlation for the second interaction virial coefficients and enhancement factors for moist air. *J. Res. Natl. Bur. Standards*, **79A,** 551–556

Hyland, R. W. and Wexler, A. 1983 Formulations for the thermodynamic properties of the saturated phases of H_2O from 173.15 K to 473.15 K. *ASHRAE Trans.*, **89,** 500–519

Jancso, G., Pupezin, J. and Van Hook, W. Al. 1970 The vapor pressure of ice between $+10^{-2}$ and -10^{+2} °C. *J. Phys. Chem.*, **74,** 2984–2989

Johari, G. P., Fleissner, G., Hallbrucker, A. and Mayer, E. 1994 Thermodynamic continuity between glassy and normal water. *J. Phys. Chem.*, **98,** 4719–4725

Kelly, K. K., Proffitt, M. H., Chan, K. R., Loewenstein, M., Podolske, J. R., Strahan, S. E., Wilson, J. C. and Kley, D. 1993 Water vapor and cloud water measurements over Darwin during the STEP 1987 tropical mission. *J. Geophys. Res.*, **98,** 8713–8723

Keyser, L. F. and Leu, M.-T. 1993 Morphology of nitric acid and water ice films. *Microscopy Res. and Technique*, **25,** 434–438

Kjaergaard, H. G., Robinson, T. W., Howard, D. L., Daniel, J. S., Headrick, J. A. and Vaida, V. 2003 Hydrated complexes of relevance to the atmosphere. *J. Phys. Chem. A*, **107,** 10680–10686

Kley, D., Russell, J. M. and Phillips, C. (Eds.) 2000 'SPARC assessment of upper tropospheric and stratospheric water vapour: WAVAS'. SPARC report No. 2, World Climate Research Programme. Available at: http://www.atmosp.physics.utoronto.ca/SPARC/Reports.html

Kohl, I., Mayer, E. and Hallbrucker, A. 2000 The glassy water–cubic ice system: A comparative study by X-ray diffraction and differential scanning calorimetry. *Phys. Chem. Chem. Phys.*, **2,** 1579–1586

Koop, T., Luo, B., Tsias, A. and Peter, T. 2000 Water activity as the determinant for homogeneous ice nucleation in aqueous solutions. *Nature*, **406,** 611–614

Kouchi, A. 1987 Vapour pressure of amorphous H_2O ice and its astrophysical implications. *Nature*, **330,** 550–552

Kraus, G. F. and Greer, S. C. 1984 Vapor pressures of supercooled H_2O and D_2O. *J. Phys. Chem.*, **88,** 4781–4785

Lin, R.-F., Starr, D. O'C., DeMott, P. J., Cotton, R., Sassen, K., Jensen, E., Kärcher, B. and Liu, X. 2002 Cirrus parcel model comparison project. Phase 1: The critical components to simulate cirrus initiation explicitly. *J. Atmos. Sci.*, **59,** 2305–2329

McDonald, J. E. 1965 Saturation vapor pressures over supercooled water. *J. Geophys. Res.*, **70,** 1553–1554

McMillan, J. A. and Los, S. C. 1965 Vitreous ice: Irreversible transformations during warm-up. *Nature*, **206,** 806–807

Marti, J. and Mauersberger, K. 1993 A survey and new measurements of ice vapor pressure at temperatures between 170 and 250 K. *Geophys. Res. Lett.*, **20,** 363–366

Mauersberger, K. and Krankowsky, D. 2003 Vapor pressure above ice at temperatures below 170 K. *Geophys. Res. Lett.*, **30**(3)**,** 1121, doi: 10.1029/2002GL016183

Mayer, E. and Hallbrucker, A. 1987 Cubic ice from liquid water. *Nature*, **325,** 601–602

Miloshevich, L. M., Vömel, H., Paukkunen, A., Heymsfield, A. J. and Oltmans, S. J. 2001 Characterization and correction of relative humidity measurements from Vaisala RS80-A radiosondes at cold temperatures. *J. Atmos. Oceanic Technol.*, **19,** 135–156

Mishima, O. and Stanley, H. E. 1998 The relationship between liquid, supercooled and glassy water. *Nature*, **396,** 329–335

Murphy, D. M. 2003 Dehydration in cold clouds is enhanced by a transition from cubic to hexagonal ice. *Geophys. Res. Lett.*, **30**(23)**,** art. No. 2230, doi: 10.1029/2003GL018566

Osborne, N. S. 1939 Heat of fusion of ice. A revision. *J. Res. Nat. Bur. Stand.*, **23,** 643–646

Osborne, N. S., Stimson, H. F. and Ginnings, D. C. 1939 Measurements of heat capacity and heat of vaporization of water in the range 0 to 100 °C. *J. Res. Nat. Bur. Stand.*, **23,** 197–260

Parsons, M. T., Mak, J., Lipetz, S. R. and Bertram, A. K. 2004 Deliquescence of malonic, succinic, glutaric, and adipic acid particles. *J. Geophys. Res.*, **109,** D06212, doi: 10.1029/2003JD004075

Poole, P. H., Sciortino, F., Essmann, U. and Stanley, H. E. 1992 Phase behaviour of metastable water. *Nature*, **360,** 324–328

Poole, P. H., Sciortino, F., Grande, T., Stanley, H. E. and Angell, C. A. 1994 Effect of hydrogen bonds on the thermodynamic behavior of liquid water. *Phys. Rev. Lett.*, **73,** 1632–1635

Pruppacher, H. R. and Klett, J. D. 1997 *Microphysics of clouds and precipitation*. Second edition. Kluwer, Dordrecht, the Netherlands

Rebelo, L. P. N., Debenedetti, P. G. and Sastry, S. 1998 Singularity-free interpretation of the thermodynamics of supercooled water. II. Thermal and volumetric behavior. *J. Chem. Phys*., **109,** 626–633

Sastry, S., Debenedetti, P. G., Sciortino, F. and Stanley, H. E. 1996 Singularity-free interpretation of the thermodynamics of supercooled water. *Phys. Rev. E*, **53,** 6144–6154

Scheel K. and Heuse, W. 1909 Bestimmung des Sättigungsdruckes von Wasserdampf unter 0 °C. *Ann. Phys*., **29,** 723–737

Smithsonian 1951 *Smithsonian Meteorological Tables*. Sixth revised edition. Ed. R. J. List. Smithsonian Institution, Washington DC, USA

2003 *Smithsonian Physical Tables*. Ninth revised edition. Ed. W. E. Forsythe. Smithsonian Institution, Washington DC, USA

Sonntag, D. 1990 Important new values of the physical constants of 1986, vapour pressure formulations based on the ITS-90, and psychrometer formulae. *Z. Meteorol*., **40,** 340–344

Speedy, R. J. 1982 Stability-limit conjecture. An interpretation of the properties of water. *J. Phys. Chem*., **86,** 982–991

Speedy, R. J. and Angell, C. A. 1976 Isothermal compressibility of supercooled water and evidence for a thermodynamic singularity at −45°C. *J. Chem. Phys*., **65,** 851–858

Speedy, R. J., Debenedetti, P. G., Smith, R. S., Huang, C. and Kay, B. D. 1996 The evaporation rate, free energy, and entropy of amorphous water at 150 K. *J. Chem. Phys*., **105,** 240–244

Starr, F. W., Angell, C. A. and Stanley, H. E. 2003 Prediction of entropy and dynamic properties of water below the homogeneous nucleation temperature. *Physica A*, **323,** 51–66

Sugisaki, M., Suga, H. and Seki, S. 1968 Calorimetric study of the glassy state. IV: Heat capacities of glassy water and cubic ice. *Bull. Chem. Soc. Jpn*, **41,** 2591–2599

Tanaka, H. 1998 Thermodynamic stability and negative thermal expansion of hexagonal and cubic ices. *J. Chem. Phys.*, **108,** 4887–4893

Tombari, E., Ferrari, C. and Salvetti, G. 1999 Heat capacity anomaly in a large sample of supercooled water. *Chem. Phys. Lett*., **300,** 749–751

Tuck, A. F., Hovde, S. J., Kelly, K. K., Reid, S. J., Richard, E. C., Atlas, E. L., Donnelly, S. G., Stroud, V. R., Cziczo, D. J., Murphy, D. M., Thomson, D. S., Elkins, J. W., Moore, F. L., Ray, E. A., Mahoney, M. J. and Friedl, R. R. 2004 Horizontal variability 1–2 km below the tropopause. *J. Geophys. Res*., **109,** D05310, doi: 10.1029/2003JD003942

Wagner, W. and Pruss, A. 1993 International equations for the saturation properties of ordinary water substance: Revised according to the international temperature scale of 1990. Addendum to *J. Phys. Chem. Ref. Data* **16,** 893 (1987). *J. Phys. Chem. Ref. Data,* **22,** 783–787

2002 The IAPWS Formulation 1995 for the thermodynamic properties of ordinary water substance for general and scientific use. *J. Phys. Chem. Ref. Data*, **31,** 387–535

Wagner, W., Saul, A. and Pruss, A. 1994 International equations for the pressure along the melting and along the sublimation curve of ordinary water substance. *J. Phys. Chem. Ref. Data*, **23,** 515–527

Washburn, E. W. 1924 The vapor pressure of ice and of water below the freezing point. *Mon. Weather Rev*., **52,** 488–490

Weber, S. 1915 Investigation relating to the vapour pressure of ice. *Community Phys. Lab. University of Leiden* **150** (data also reproduced in Spencer-Gregory H. and Rourke E., 1957, *Hygrometry*, Crosby Lockwood and Son, London, UK)

Wexler, A. 1976 Vapor pressure formulation for water in range 0 to 100 °C. A revision. *J. Res. Natl. Bur. Stand. Sect. A*., **80,** 775

1977 Vapor presure formulation for ice. *J. Res. Natl. Bur. Stand. A*., **81,** 5–20

Wexler, A. and Hyland, R. 1983 A formulation for the thermodynamic properties of the saturated pure ordinary water-substance from 173.15 to 473.15 K. In *Thermodynamic properties of dry air, moist air, and water and SI psychrometric charts.* Project 216. Special publication of the American Society of Heating, Refrigerating and Air-Conditioning Engineers, Atlanta, USA

Wexler, A. S. and Clegg, S. L. 2002 Atmospheric aerosol models for systems including the ions H^+, NH_4^+, Na^+, SO_4^{2-}, NO_3^-, Cl^-, Br^- and H_2O. *J. Geophys. Res.*, **107,** D14, art. no. 4207, 2002. (On-line aerosol inorganics model: http://www.hpc1.uea.ac.uk/∼e770/aim.html or http://mae.ucdavis.edu/wexler/aim.htm)

WMO 1988 'General meteorological standards and recommended practices, appendix A'. Technical Regulations, WMO-No. 49. World Meteorological Organization, Geneva, Switzerland

2000 'General meteorological standards and recommended practices'. Corrigendum to 1988 edition. WMO-No. 49. World Meteorological Organization, Geneva, Switzerland

Wright, J. M. 1997 Rawinsonde and Pibal observations. In *Federal meteorological handbook No. 3*. FCM-H3-1997. Office of Federal Coordinator for Meteorological Services and Supporting Research (OFCM), Washington DC, USA